Heterogeneous photochemistry of dicarboxylic acids on mineral dust

Milena Ponczek, Nathalie Hayeck, Corinne Emmelin, C. George

▶ **To cite this version:**

Milena Ponczek, Nathalie Hayeck, Corinne Emmelin, C. George. Heterogeneous photochemistry of dicarboxylic acids on mineral dust. Atmospheric Environment, 2019, 212 (—), pp.262-271. 10.1016/j.atmosenv.2019.05.032 . hal-02275912v1

HAL Id: hal-02275912

https://hal.science/hal-02275912v1

Submitted on 1 Dec 2019 (v1), last revised 29 Jan 2020 (v2)

HAL is a multi-disciplinary open access archive for the deposit and dissemination of scientific research documents, whether they are published or not. The documents may come from teaching and research institutions in France or abroad, or from public or private research centers.

L'archive ouverte pluridisciplinaire **HAL**, est destinée au dépôt et à la diffusion de documents scientifiques de niveau recherche, publiés ou non, émanant des établissements d'enseignement et de recherche français ou étrangers, des laboratoires publics ou privés.

Heterogeneous photochemistry of dicarboxylic acids on mineral dust

Milena Ponczek, Nathalie Hayeck[&], Corinne Emmelin, Christian George*

Univ Lyon, Université Claude Bernard Lyon 1, CNRS, IRCELYON, F-69626, Villeurbanne, France

[&] Now at the Chemistry Department, Faculty of Arts and Sciences, American University of Beirut, Beirut, Lebanon

*correspondence to: christian.george@ircelyon.univ-lyon1.fr

Abstract

Dicarboxylic acids have low volatilities and hence are present mostly in the particulate phase, including the surface of dust particles. Mineral dust, globally the most emitted aerosol, has photocatalytic properties that can initiate photo-induced heterogeneous chemistry of organic compounds, which is still poorly characterized. We investigated the photochemistry of five dicarboxylic acids (DCA) i.e., succinic (butanedioic) acid, glutaric (pentanedioic) acid, adipic (hexanedioic) acid, pimelic (heptanedioic) acid and suberic (octanedioic) acid on Arizona test dust (ATD) particles upon UV-A light irradiation (0 – 1.4 mW cm^{-2}). Gas-phase products were monitored by a high-resolution proton-transfer-reaction mass spectrometer (PTR-ToF-MS), and surface sorbed products were extracted and analyzed by ultra-high-performance liquid chromatography coupled to a heated electrospray ionization high-resolution mass spectrometer (UHPLC-HESI-HRMS). Monoacids and aldehydes were the main observed and quantified gaseous products. In contrast, shorter chain DCA and highly oxygenated products were found at the surface of the dust particles. Interestingly, the photochemistry of these DCAs presented an even-odd alternation concerning their heterogeneous reactivity, with odd-numbered carbon diacids being more reactive than their even-numbered homologous ones. We present and discuss a reaction mechanism for the C_4-C_8 DCA heterogeneous photooxidation catalysed by TiO_2/Fe_2O_3-rich dust particles. Our results suggest that photochemical processing on dust surfaces should be regarded as a possible efficient pathway for altering their surface properties impacting ice nucleation and cloud condensation properties.

1 Introduction

Dicarboxylic acids (DCA) are ubiquitous in the atmosphere and are especially abundant in aerosols (Kawamura and Bikkina, 2016). In fact, due to the presence of two carboxylic groups, they are less volatile and more soluble in water when compared to the respective monoacids. Oxalic acid (C_2) is the most abundant diacid, followed by malonic (C_3) and succinic (C_4) acids (Kawamura et al., 1996). Dicarboxylic acids and related compounds (oxo and keto acids, and other dicarbonyls) are emitted from anthropogenic and natural primary sources such as fossil

fuel combustion, biomass burning, cooking, and oceans. They are also widely used in hydraulic fluids, agricultural chemicals, pharmaceuticals, dyes, complexing agents, and as intermediates in the manufacture of esters and polyamides (Helmi Rozaini, 2012), increasing the possibilities of fugitive emissions during transportation or storage. Although direct emissions contribute to the diacids abundance, several studies have shown that low molecular weight (LMW) diacids are also produced in the troposphere by photochemical chain reactions implying unsaturated hydrocarbons and fatty acids, as well as their oxidation products (Kawamura et al., 1996; Kawamura and Ikushima, 1993; Kawamura and Yasui, 2005). These results are supported by the observation of diurnal and seasonal variation where an increase of DCA concentration in the afternoon and summer times coincides with higher levels of atmospheric oxidants (Kawamura and Bikkina, 2016).

Except for the ketoacids, carboxylic acids do not absorb significantly at wavelengths greater than 250 nm, and generally, do not undergo photolysis in the troposphere (Mellouki et al., 2015). Additionally, they have weak reactivity in the gaseous phase, thus, their removal from the atmosphere is mainly through heterogeneous processes (i.e., dry and wet depositions) (Chebbi and Carlier, 1996). Water-soluble C_2–C_9 DCAs have low vapor pressure which favors their adsorption onto airborne particles (Yang et al., 2008), including mineral aerosols, particularly over Asia or over oceans (Pan et al., 2017; Sullivan et al., 2007). Indeed, Russell et al. reported the presence of complex mixtures of carbonyl compounds on dry particles from the Caribbean marine boundary layer (Russell et al., 2002). Corroborating this result, oxalic acid was found in Asian mineral dust particles for both sub and super-micron diameters (Sullivan and Prather, 2007). Oxalic, succinic, malic, glutaric and adipic acids were also shown to be adsorbed on mineral dust particles collected in Israel (Falkovich et al., 2004). Moreover, the presence of DCA alters mineral dust hygroscopic properties (Russell et al., 2002), and consequently their possible ability to act as ice nucleation and cloud condensation nuclei (Keskinen et al., 2014; Niedermeier et al., 2010; Tang et al., 2016).

Mineral dust is the most abundant emitted aerosol accounting for a range between 1000-3000 Tg released into the atmosphere every year (Formenti et al., 2011). Recently, the photo-induced heterogeneous chemistry initiated by near-UV/Vis light-absorbing species (such as TiO_2, Fe_2O_3) present in mineral aerosol was evinced (Ndour et al., 2009; Ponczek and George, 2018; Romanias et al., 2016; Styler and Donaldson, 2012, 2011) and reviewed (Chen et al., 2012; George et al., 2015; Usher et al., 2003). All these studies reveal a new and potentially important pathway of organic compounds processing in the atmosphere.

There are few studies of the kinetics and products identification for the atmospheric photooxidation of aqueous phase chemistry of dicarboxylic acids (Charbouillot et al., 2012; Pavuluri et al., 2015; Yang et al., 2008). However, similar knowledge for heterogeneous reactions on typical mineral dust is still very limited. In this study, we assessed the photoreactivity of five dicarboxylic acids namely, succinic (butanedioic) acid, glutaric (pentanedioic) acid, and adipic (hexanedioic) acid, pimelic (heptanedioic) acid and suberic (octanedioic) acid on Arizona test dust (ATD) particles. The heterogeneous processing on the dust surface was investigated under

UV-A irradiation. We discussed the similarities and discrepancies among these homologous compounds and proposed a general mechanism for DCA reactions on ATD.

2 Experimental Section

Experiments were carried out in a horizontal coated wall flow tube reactor, previously described in detail (Jammoul et al., 2008; Ponczek and George, 2018), where the acid-coated dust samples were immobilized on the internal walls of a Pyrex tube insert. The reactor had an outer jacket and was maintained at a constant temperature of 293 K by circulating thermostated water from a chiller bath (Huber CC 130). Seven lamps (Phillips 20W) surround the reactor and could be switched on and off modifying the light intensity (from 0 to 1.4 mW cm^{-2} for wavelengths in the range of 300-400 nm). A schematic of the experimental set-up is depicted in**Figure *1***.

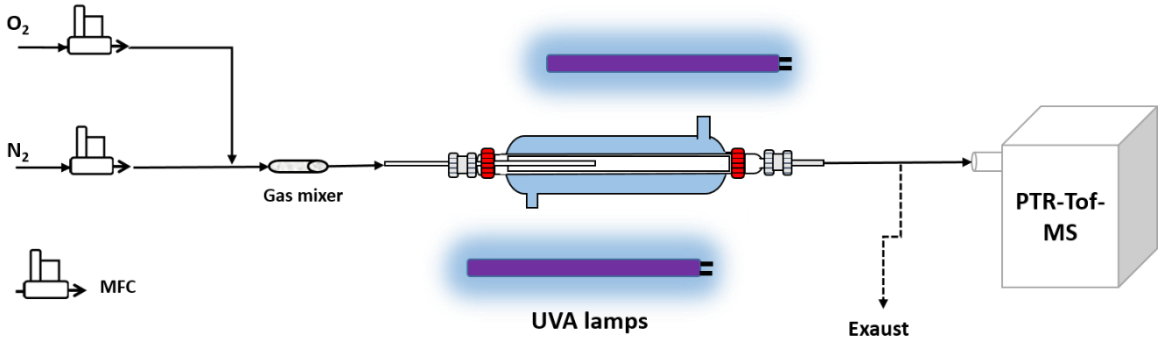

Figure 1: Schematic of experimental set-up

2.1 Sample preparation and tube coating

All chemicals were used as received without any further treatment. Succinic, Glutaric and Adipic acids were purchased from Sigma Aldrich (>99%for all); Pimelic (>98%) and Suberic acids (99%) were purchased from Alfa Aesar, Arizona test dust, a real sand from Salt River Valley, Arizona, U.S., was commercially provided by Powder Technology Inc. (ISO 12103-1, A1 Ultrafine Test Dust, ATD); it is well-characterized regarding its composition and chemical and thermal stability (Cwiertny et al., 2008; Vlasenko et al., 2005). ATD composition is shown in the Supplement Material.

To prepare the DCA coated dust samples, acids were added as internal mixtures during the coating process at a 10% w/w ratio in ATD. To do so, an aqueous solution of the respective acid was mixed with an ATD suspension in ethanol (absolute, 99% Sigma Aldrich). The final suspension was then transferred to the tube inserts coating their inner walls, similar to the coating process described previously (Ponczek and George, 2018). The tubes were left in an oven at 373 K for 1 h to evaporate the solvents (ethanol and water) except the DCA which boiling points are between 473 and 673 K.

2.2 Experiment procedure

After coating, the freshly prepared insert was placed in the flow tube reactor, under a flow of 300 ml min^{-1} of synthetic air (N_2 and O_2 mixture in the ratio 79:21) as a carrier gas. To investigate photooxidation reactions, each sample followed the same illumination sequence: 30 min off (for background measurement); 1 h under irradiation, 1 h lights off, 1 h under irradiation.

The gas-phase products were monitored online by coupling the reactor outlet to a high-resolution proton-transfer-reaction mass spectrometer (PTR-ToF-MS 8000, Ionicon Analytik GmbH). The instrument settings used were: drift voltage of 600 V, drift temperature of 333 K and drift pressure of 2.42 mbar, resulting in an E/N ratio of about 125 Td (1 Td = 10^{-17} V cm^2). The reactor's outlet and the PTR sample inlet tubing were constantly heated to 333 K to minimize adsorption and loss of products. Spectra were acquired at a time resolution of 5 s for regular experiments and 10 s for the long-term experiments. VOC mixing ratios were calculated from the H_3O^+ mode using the built-in feature of PTR-ToF-MS Viewer Software v. 3.1.0.31 (Ionicon Analytik GmbH), considering default values for the proton transfer reaction rate constant (k = 2 x 10^{-9} cm^3 s^{-1}) for all VOCs. It should be noted that uncertainties in the absolute mixing ratios can be estimated to be about 30% (Brüggemann et al., 2017; Hartungen et al., 2004).

2.3 Surface Products – Sample Extraction and LC-MS Analysis

After irradiation, surface sorbed products were extracted from the dust as follows. First, 10 ml of solvent (9:1 v/v of acetonitrile–water - Optima® LC/MS, Fischer Scientific, USA) was added to the coated tube and sonicated for 10 min. Then, the suspension in the tube was left in a rotating device overnight (for approx. 15 h) providing good contact solvent–dust. After that, the suspension was transferred to a 30 mL amber vial and left to decant. The supernatant was, next, transferred to another amber vial and filtered using 0.2 μm GHP membrane (13 mm, Pall Corporation, USA), and evaporated almost to dryness under a mild nitrogen flow. The extracts were then reconstituted in 1 mL of a 50:50 volume mixture of water and acetonitrile (ACN).

For the analysis, the appropriate amount of the final reconstituted extract sample (see Table S1) was diluted by adding 500 μL of acetonitrile and 500 μL of water. 5 μL of diluted solutions were analyzed by reversed phase ultra-high-performance liquid chromatography UHPLC (Dionex 3000, Thermo Scientific, USA) coupled to an Orbitrap high-resolution mass spectrometer (Thermo Scientific, USA) using heated negative electrospray ionization (- HESI). Each sample was analysed in triplicate.

Analytes were separated using a Waters Acquity HSS T3 column (1.8 μm, 100 × 2.1 mm) with mobile phases consisting of (A) 0.1% formic acid in water (Optima® LC/MS, Fischer Scientific, USA) and (B) 0.1% formic acid in acetonitrile (Optima® LC/MS, Fischer Scientific, USA). Gradient elution was performed by the A/B mixture at a total flow rate of 300 μL min^{-1} as detailed elsewhere (Wang et al., 2016). Further information regarding the chromatographic and mass spectrometric methods is available in the Supplementary Material.

The chromatograms were analyzed with MZMine 2.21 for a non-target screening of potential products. The software algorithm identifies the products assuming that the extracted ions in the range of 50–750 *m/z* were formed by the loss of a proton from the analytes; adducts formation with acetonitrile ($[M+ACN]^-$) was also verified. To refine these results, the major products identified by MZMine were re-evaluated and each corresponding peak was manually checked using the software Xcalibur 2.2 (Thermo, USA), thus excluding possible peaks detected erroneously by the automatic screening.

Chromatograms of each sample (extracted from the irradiated tube after the experiment) were compared to the results of a replicate tube prepared under the same conditions but left in the dark. Additionally, two procedural blanks consisting of coated tubes with only Arizona test dust (and no acid) one left in the dark and the other irradiated were run in parallel to the samples.

Standard solutions of the studied acids were also analyzed to validate their identification in the samples using their corresponding retention time in addition to the high-resolution mass spectra. Experiments using succinic acid have not been analysed by LC-MS since this acid is too small and too polar to be sufficiently retained by our C18-column, as probably are its oxidation products.

3 Results and Discussion

For all dicarboxylic acids / ATD films, illumination resulted in the immediate increase of various signals detected by the PTR-ToF-MS. However, each acid presented different time responses, product distributions and yields. Typical results for glutaric (C_5) and adipic (C_6) acids are shown in Figure 2.

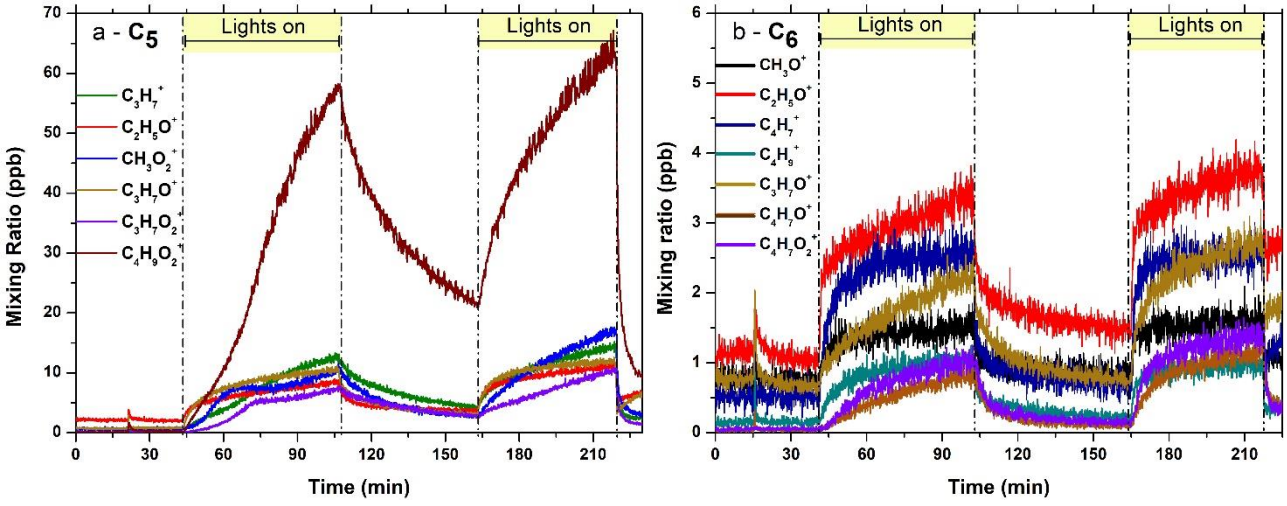

Figure 2: Gas-phase products observed by PTR-ToF-MS for irradiated ATD films coated with (a) Glutaric acid (C_5) and (b) Adipic acid (C_6)

We can observe from Figure 2, that glutaric (C_5) and adipic (C_6) acids presented very different OVOCs (oxygenated volatile organic compounds) production profiles. Glutaric acid had a main product $C_4H_9O_2^+$ (*m/z* 89.059), which increased rapidly and reached concentrations above 50 ppb. While for adipic acid, we did not observe a foremost compound and products were more evenly distributed. The mixing ratios time profiles for succinic (C_4), pimelic (C_7) and suberic (C_8) acids are presented in the Supplement Material (left side of Figure S2). It is remarkable that some products easily reached steady state, such as $C_4H_7^+$ for adipic acid (C_6) and $C_3H_7O^+$ for suberic acid (C_8), whereas others exhibited almost linear increasing during one-hour irradiation i.e., $C_4H_9O_2^+$ for glutaric acid (C_5) and $C_5H_{13}O_2^+$ for pimelic acid (C_7). Interestingly, some of them dropped-off quite fast after switching off lights ($C_4H_7O_2^+$ for adipic acid and $C_5H_9^+$ for pimelic acid), while others decayed very slowly ($C_3H_7^+$ for glutaric acid and $C_2H_5O^+$ for adipic acid). Moreover, during the same experiment, when the lights were switched on for the second time, the same products were observed, but with different time profiles. Overall, about 50 different *m/z* ions were identified and the complete list of all detected VOCs is given in Table S2.

Although the PTR-ToF-MS has a high mass resolution (more than 4000 m/Δm), allowing to differentiate compounds with very close *m/z* e.g., ethanol ($C_2H_7O^+$, *m/z* 47.049) and formic acid ($CH_3O_2^+$, *m/z* 47.013), small ions such as $C_3H_5^+$ (*m/z* 41.039), $C_2H_3O^+$ (*m/z* 43.018), $C_3H_7^+$ (*m/z* 43.054), $C_4H_9^+$ (*m/z* 57.069), will have contributions from different fragments in a complex mixture. Fragmentation patterns for atmospherically relevant OVOCs have already been studied and recently reviewed (Yuan et al., 2017), but it may be altered depending on the actual experimental conditions (for example, humidity) and instrument settings (de Gouw and Warneke, 2007). In an attempt to improve product identification, we measured pure standards for some monocarboxylic acids (butanoic, pentanoic, heptanoic and octanoic) and aldehydes (Ponczek and George, 2018). We found out that under our operational conditions, the parent molecule MH^+ is approximately, 77% of the relative intensity. Fragments related to the loss of one molecule of water ($[MH^+] - H_2O$) and, one molecule of water and one group CO ($[MH^+] - H_2O$ - CO) were also found, whereas these two alternative fragmentation channels were more variable, between 5-10% for ($[MH^+] - H_2O$) and between 5 and 20% for ($[MH^+] - H_2O$ - CO) depending on the acid.

Control experiments were performed to verify that the OVOCs detected were emitted solely from the photo-induced process and not as a result of i) evaporation from the dicarboxylic acid or; ii) due to the presence of impurities on the dust. For this, acid/dust coated inserts were subject to the same experimental conditions and left overnight in the dark while the concentration of VOC was monitored. Also, dust films without any acid were submitted to the same irradiation procedure. In both cases, no significant difference in OVOCs concentrations was detected.

The net product formation was quantified by considering the first hour of irradiation and subtracting the baseline values as measured before irradiation. This net product formation is presented in Figure 3 for glutaric (C_5) and adipic (C_6) acids, and in Figure S2 (right side) for succinic (C_4), pimelic (C_7) and suberic (C_8) acids. In both

figures, error bars were calculated from three replicates. The mass variability of dust films was not an issue for the reproducibility of the results as it can be observed in Figure S3. Therefore, the relative abundance (RA_{VOC}) of each VOC was calculated with respect to the total of VOCs emitted ΔC_{Total}, Eq. 1:

$$RA_{VOC_A}(\%) = \frac{\Delta C_A}{\Delta C_{Total}} x\ 100\ , \quad (1)$$

where ΔC_A is the mixing ratio of the respective VOC emitted (subtracting the values of the baseline signal), and ΔC_{Total} is the sum of all VOC emitted ($\sum \Delta C_A\ for\ all\ products$).

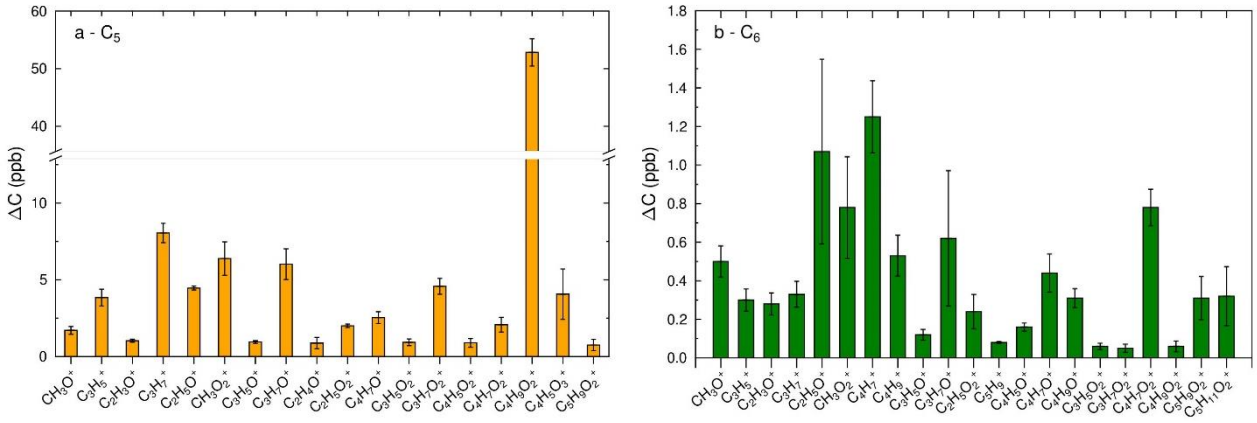

Figure 3: Net product formation for (a) Glutaric acid (C_5) and (b) Adipic acid (C_6) after 1h irradiation. The error bars represent the standard deviation of three replicates, evidencing the reproducibility of the results.

The relative abundance, as well as the formula assignment and identification of the three foremost gas-phase products for each dicarboxylic acid, is shown in Table 1. It can be observed that monocarboxylic acids and aldehydes are the most common products of diacids photooxidation. Formic acid, the simplest (monocarboxylic acid) MCA appeared for succinic (C_4), glutaric (C_5) and pimelic (C_7) acids with similar relative abundances, while acetaldehyde appeared as a major product for succinic (C_4), adipic (C_6) and suberic (C_8) acids although its relative abundance for succinic acid was much higher than for the other two diacids.

It is worth pointing out that the detection of gaseous products depends not only on their formation reaction rates but also on their adsorption/desorption properties at the surface; besides, OVOCs interact differently with oxides components of ATD (Carlos-Cuellar et al., 2003; Li et al., 2001). For instance, more volatile compounds, such as small aldehydes will preferentially desorb, and molecules liable to hydrogen bonds may become more strongly bounded to dust surface hydroxyl groups (Chen et al., 2012; Styler et al., 2013). Therefore, some products may desorb more easily than others, while some of them must remain adsorbed to further oxidation. This point is further discussed in the discussion of the mechanism (Sec. 3.5).

Table 1: Main gas-phase products for each dicarboxylic acid, where ΔC is the net product formation on mixing ratio units (ppb) of the respective VOC emitted and RA is the respective relative abundance (Eq. 1). The standard deviation (Std Dev) was calculated for three replicates.

Starting DCA	Products						
	m/z	Formula	Suggested product	ΔC (ppb)	Std Dev (ppb)	RA (%)	Std Dev RA(%)
Succinic C_4	45.033	$C_2H_5O^+$	Acetaldehyde	9.44	1.99	59.5%	8.4%
	75.042	$C_3H_7O_2^+$	Propanoic acid	1.60	1.00	10.0%	5.7%
	47.011	$CH_3O_2^+$	Formic acid	1.12	0.35	7.1%	2.3%
Glutaric C_5	89.059	$C_4H_9O_2^+$	Butanoic Acid	52.82	2.37	50.1%	0.7%
	47.011	$CH_3O_2^+$	Formic acid	6.39	1.09	6.1%	1.0%
	59.049	$C_3H_7O^+$	Propanal	6.02	1.00	5.7%	1.0%
Adipic C_6	55.054	$C_4H_7^+$	Butyraldehyde	1.25	0.19	14.7%	0.7%
	45.033	$C_2H_5O^+$	Acetaldehyde	1.07	0.48	12.3%	4.1%
	87.042	$C_4H_7O_2^+$	Crotonic Ac/ Succialdehyde	0.78	0.09	9.2%	1.4%
Pimelic C_7	69.069	$C_5H_9^+$	Pentanal	3.74	0.65	16.6%	0.4%
	117.091	$C_6H_{13}O_2^+$	Hexanoic Acid	3.37	1.26	14.6%	3.3%
	47.011	$CH_3O_2^+$	Formic Acid	1.68	0.30	7.5%	1.0%
Suberic C_8	83.084	$C_6H_{11}^+$	Hexanal	1.58	0.59	20.6%	4.7%
	45.033	$C_2H_5O^+$	Acetaldehyde	0.85	0.12	11.4%	2.3%
	55.053	$C_4H_7^+$	Butyraldehyde	0.84	0.27	10.9%	1.9%

3.1 Light Intensity Dependence

The influence of light intensity on the product formation and yield was investigated by varying the number of lamps switched on, decreasing the radiant flux (300-400 nm) from 1.4 to 0.40 mW cm^{-2}. Figure 4 illustrates the concentration profiles and the quantification of products of a succinic acid/ATD coated film at different light intensities.

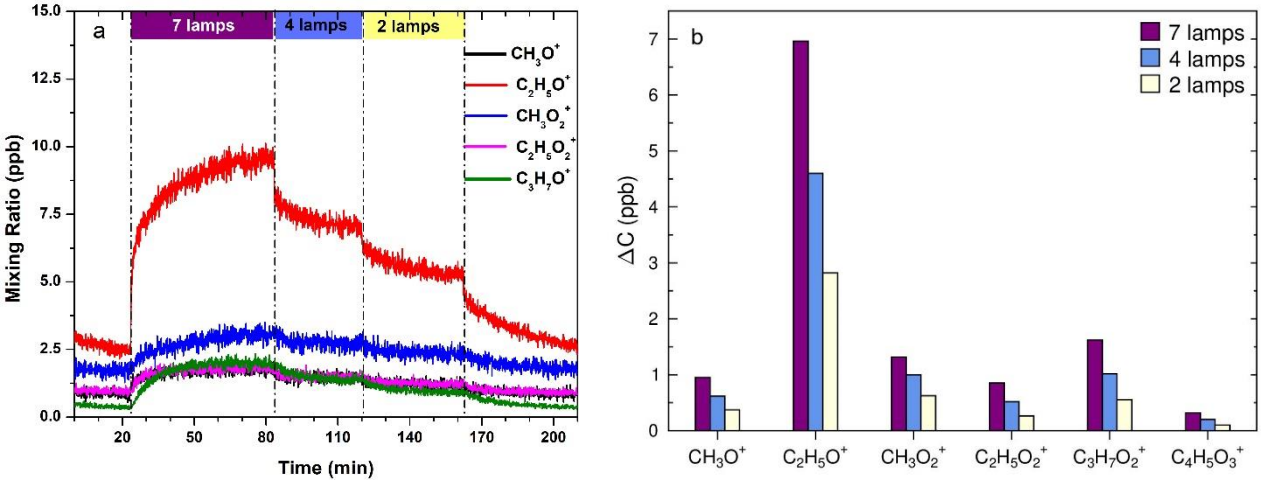

Figure 4: Light influence on product mixing ratios for succinic acid (C_4): (a) temporal profile and (b) net product quantification. The number of lamps switched on (2, 4 or 7) is indicated by the colors in the legend.

As the light intensity decreased, the concentration of products decreased visibly; the same behavior was observed for all the other DCA experiments. This observation highlights the photo-induced nature of the reaction occurring on ATDs surface since photocatalytic reaction rates are usually proportional to the radiant flux for low/moderate illumination intensities (Herrmann, 2010). For the region where the reaction rate is linearly proportional to the radiant flux, the formation of photogenerated holes (h^+) could be the limiting step (Herrmann, 2001; Ohtani, 2010), and once formed, they must react with an electron donor.

3.2 Long-term Irradiation Experiments

As shown in Figure 5, the emission of several VOCs is sustained up to 14 hours of continuous illumination for a film of ATD and pimelic acid (C_7). When the lights were turned off, the flow of all VOCs decayed, instantly. In addition, it is possible to follow the time evolution of products: while some of them such as $C_6H_{13}O_2^+$ (*m/z* 117.090) and $C_5H_{11}O_2^+$ (*m/z* 103.073) proceed towards steady state after some hours, others such as $C_2H_5O^+$ (*m/z* 45.033), $C_4H_7O^+$ (*m/z* 71.048) and $C_4H_7O_2^+$ (*m/z* 87.044) increase continuously throughout the irradiation period. $C_5H_9^+$ (*m/z* 69.069) reaches a maximum after 1 h and then, slowly decreases. The same tendency for different products was observed in the experiments with other dicarboxylic acids. According to the different time evolution of the detected products we observed, for instance, that for pimelic acid (C7) $C_6H_{13}O_2^+$ and $C_5H_{11}O_2^+$ that correspond to monocarboxylic acids reached steady state, whereas $C_2H_5O^+$, $C_4H_7O^+$ and $C_4H_7O_2^+$ which correspond to aldehydes continue to increase their concentrations. This observation shed light in the elucidation of the mechanism where the C_{n-1} monoacidcarboxylic acids are produced first, while the aldehydes are produced in steps later.

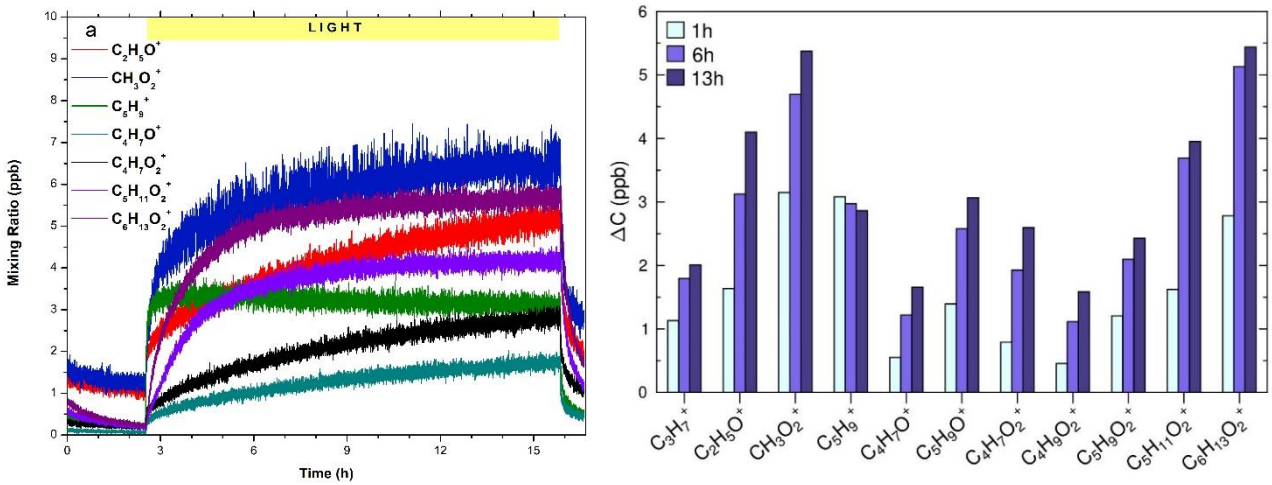

Figure 5: Gas-phase products – Long-term Irradiation for Pimelic Acid (C_7). (a) Mixing ratio temporal profile and (b) net product distribution for 1h, 6 h and 13h of illumination.

3.3 Even-Odd alternation of diacids reactivity

Figure 6**Erreur ! Source du renvoi introuvable.** presents the total gas-phase product mixing ratio i.e., the sum of all VOCs emitted ($\sum \Delta C_A \ all\ products$) for 1 hour of irradiation for each dicarboxylic acid studied as a function of the number of carbons, showing a clear alternation of reactivity between even and odd compounds. Odd-carbon DCA exhibit higher reactivity than the even-carbon analogous ones.

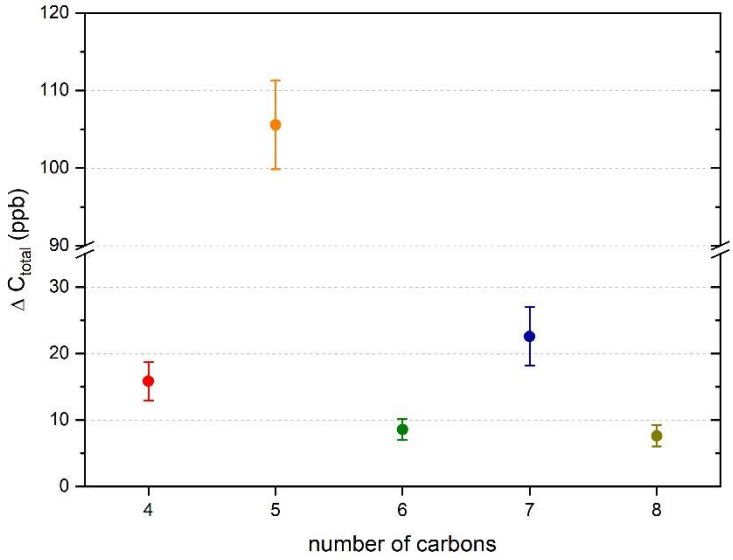

Figure 6: Total gas-phase products mixing ratio after 1h of irradiation for all five dicarboxylic acids studied, as a function of carbons number in DCA molecules. Error bars represent the standard deviation for three replicates.

Several studies report odd-even alternation of solid-state physical properties of diacids, namely, saturation vapor pressure (Bilde et al., 2015), melting point (Thalladi et al., 2000), solubility in water (Zhang et al., 2013) and in organic solvents (Zhang et al., 2014). Odd-carbon DCAs are more soluble, have higher vapor pressure, lower melting point and sublimation enthalpy. Recently, the odd/even alternation behavior on chemical reactivity was

reported by Fairhurst and coworkers (Fairhurst et al., 2017) and, Zhao et al (2017) (Zhao et al., 2017) respectively, in the reactive uptake on solid C_3–C_8 diacids films and chemical reactivity of submicron C_3–C_7 dicarboxylic acid particles with gas-phase amines.

Concerning photooxidation reactions in the homogeneous liquid-phase, Yang and coworkers (Yang et al., 2008) examining the oxidation kinetics and mechanisms of C_2–C_9 DCAs by OH-radical, observed the monotonic increase of DCAs degradation rate constant as a function of carbon numbers (for a number of carbons > 4) and no alternation was reported. On the other hand, Sun et al. (Sun et al., 2014) observed the same odd/even fluctuation on reactivity as reported herein, for TiO_2-based heterogeneous liquid-phase photocatalytic degradation of C_2-C_6 dicarboxylic acids. ATR-IR spectra indicated that malonic acid adsorbed on TiO_2 from an aqueous solution in the dark exhibited two different carboxylate groups adsorption geometries (Dolamic and Bürgi, 2006). Later, the same authors (Dolamic and Bürgi, 2007) compared ATR-IR vibration bands of malonic (C_3) and succinic (C_4) and proposed different adsorption modes for each acid since for succinic acid both carboxylic groups were equivalent. Sun and coworkers (Sun et al., 2014) confirmed different surface adsorption geometry for glutaric (C_5) and succinic acids(C_4). For odd-DCAs, one carboxylic group adopt monodentate coordination and the other, bidentate coordination with TiO_2 surface; whereas, for even-DCAs, the two carboxylic groups exhibit the same bidentate bridging coordination. These observations can explain the differences between homogeneous and heterogeneous photooxidation mechanisms of dicarboxylic acids.

In Table 1, it can be seen that the odd-numbered diacids mostly produced the $C_{(n-1)}$ monocarboxylic acid and formic acid whereas even-DCAs mainly produced aldehydes. Succinic acid (C_4), however, even having as primary product acetaldehyde, also produced propanoic and formic acids, whereas the other even-numbered-DCAs did not produce MCA in detectable amounts in the gas phase. Another remarkable observation was the fact that glutaric (C_5) and pimelic (C_7) acid samples showed a very strong odor after irradiation indicating the production of odorous compounds (such as butanoic and hexanoic acids) in concentrations perceptible to the human nose. The even-carbon DCAs tubes did not exhibit any strong odor.

3.4 Surface products

To better understand the mechanism and possible differences between the odd and even compounds, we analyzed by UHPLC / (-) HESI-MS the extracts of products that remained adsorbed on the mineral surface. In Figure 7 we compare the irradiated sample chromatogram of pimelic acid, adipic acid, and glutaric acid (C_7, C_6 and C_5, respectively) experiments to three respective blanks: the pure extraction solvent mixture [Blc Solv], a pure ATD irradiated tube[Pure ATD_IRR], a sample from dust containing the same acid but kept in the dark [ATD_DCA_D].

Succinic acid (C_4) (*m/z* 117.0190) was found as major surface-product from glutaric acid (C_5) reaction. Glutaric acid (*m/z* = 131.0349) was found in the adipic acid (C_6) experiment sample, and the ion *m/z* = 145.0503 corresponding to adipic acid was observed in the pimelic acid (C_7) sample. Diacids identification was made by

comparison with standard solutions in concentrations equivalent to those found in the samples. As observed in Figure 7, the mentioned products were only found in the irradiated sample containing the corresponding DCA.

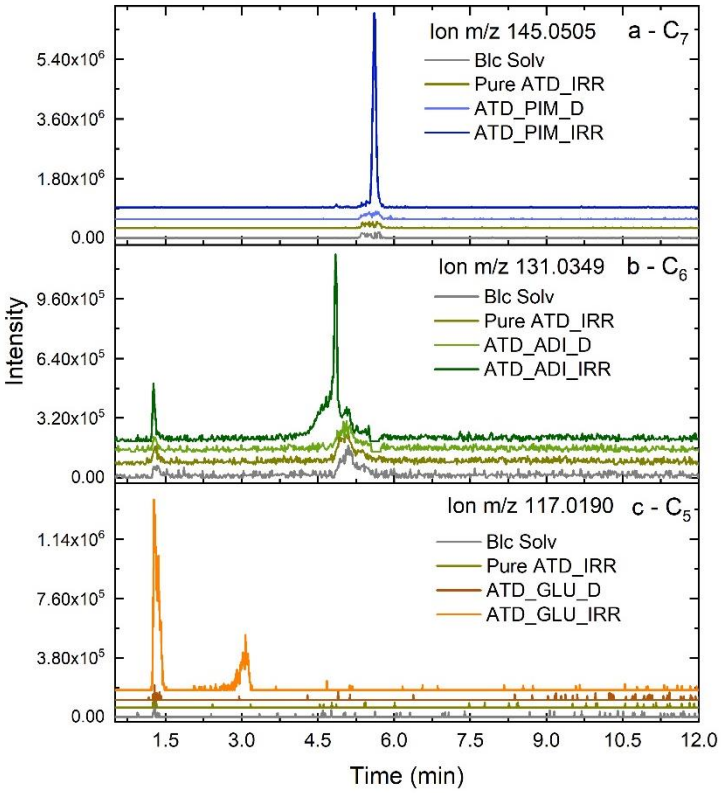

Figure 7: Chromatograms obtained for diacids surface products, following extracted ions as indicated, comparing the irradiated samples [ATD_DCA_IRR] to the blanks (pure extraction solvent [Blc Solv], pure ATD irradiated [Pure ATD_IRR] and the corresponding diacid/ATD sample kept in the dark [ATD_DCA_D]); for (a) pimelic acid (C_7) sample, ion *m/z* = 145.0503; (b) adipic acid (C_6) sample, ion *m/z* = 131.0349; (c) glutaric acid (C_5) sample, ion *m/z* = 117.019.

The dicarboxylic acid $C_{(n-1)}$ appeared as an adsorbed product for all four diacids analysed by LC-MS; in the case of glutaric (C_5), adipic (C_6) and pimelic acids (C_7) (chromatograms shown in Figure 7), they were also the most abundant surface product. Many other organic compounds, which are not sufficiently volatile to desorb from the surface, have been detected in the sorbed phase. The integrated peak areas for some compounds identified for adipic (C_6), pimelic (C_7) and suberic (C_8) acids experiments are shown in Figure S4 for the irradiated samples compared to the dark ones in order to evidence the relative abundance of the products generated under illumination.

These results indicate that the photooxidation mechanism of dicarboxylic acids results in the diacid $C_{(n-1)}$ suggesting their decarboxylation is an important step. Also, other highly oxygenated products such as ($C_nH_{2n-2}O_3$), ($C_mH_{2m}O_3$), ($C_mH_{2m}O_4$), etc. were found, Table 2. It should be pointing out the appearance of molecules of greater molecular weight than the original acid suggests dimerization or recombination of radicals throughout photooxidation.

Table 2: List of the main condensed phase compound classes of products when glutaric, adipic, pimelic or suberic acids ATD films were exposed to light. Most abundant products are highlighted in bold.

General Formula	Proposed Function	Glutaric *(C_5)*	Adipic *(C_6)*	Pimelic *(C_7)*	Suberic *(C_8)*
$C_mH_{2m-2}O_2$	dialdehyde			$C_6H_{10}O_2$	$C_6H_{10}O_2$
$C_mH_{2m-2}O_3$	**Oxo or keto acid**	**$C_4H_6O_3$**	**$C_5H_8O_3$, $C_4H_6O_3$**	**$C_6H_{10}O_3$**	**$C_7H_{12}O_3$** **$C_6H_{10}O_3$**
$C_mH_{2m-2}O_4$	**DCA**	**$C_4H_6O_4$**	**$C_5H_8O_4$**	**$C_6H_{10}O_4$, $C_5H_8O_4$**	**$C_7H_{12}O_4$**
$C_mH_{2m-2}O_5$	OH-DCA			$C_6H_{10}O_5$	
$C_mH_{2m-4}O_6$			$C_{10}H_{16}O_6$	$C_{12}H_{20}O_6$	
$C_mH_{2m}O_3$	**OH-MCA**	**$C_4H_8O_3$**	**$C_5H_{10}O_3$**	**$C_6H_{12}O_3$**	**$C_6H_{12}O_3$**
$C_mH_{2m}O_4$	**Di-OH-MCA**		**$C_5H_{10}O_4$**	**$C_6H_{12}O_4$**	**$C_7H_{14}O_4$**
$C_mH_{2m-4}O_4$	unsat DCA	$C_5H_6O_4$		$C_7H_{10}O_4$ $C_{11}H_{18}O_4$	
$C_mH_{2m-4}O_5$	oxo-DCA		$C_6H_8O_5$	$C_7H_{10}O_5$, $C_6H_8O_5$, $C_{12}H_{20}O_5$	$C_8H_{12}O_5$
$C_mH_{2m-4}O_6$			$C_{11}H_{18}O_6$, $C_{10}H_{16}O_6$		

3.5 Mechanistic Insights

Taking into consideration the results presented previously for the products observed in the gas and sorbed phases and also their relative abundances, a general mechanism is proposed for dicarboxylic acids photo-oxidation (Figure 8). It is worthwhile to mention that the reactivity of mineral dust is attributed, and assumed for the mechanism presented herein, to the content of semiconductor materials generally present in variable amounts. ATD, specifically, contains 2.0 – 5.0 wt% Fe_2O_3 and 0.5 – 1 wt% TiO_2.

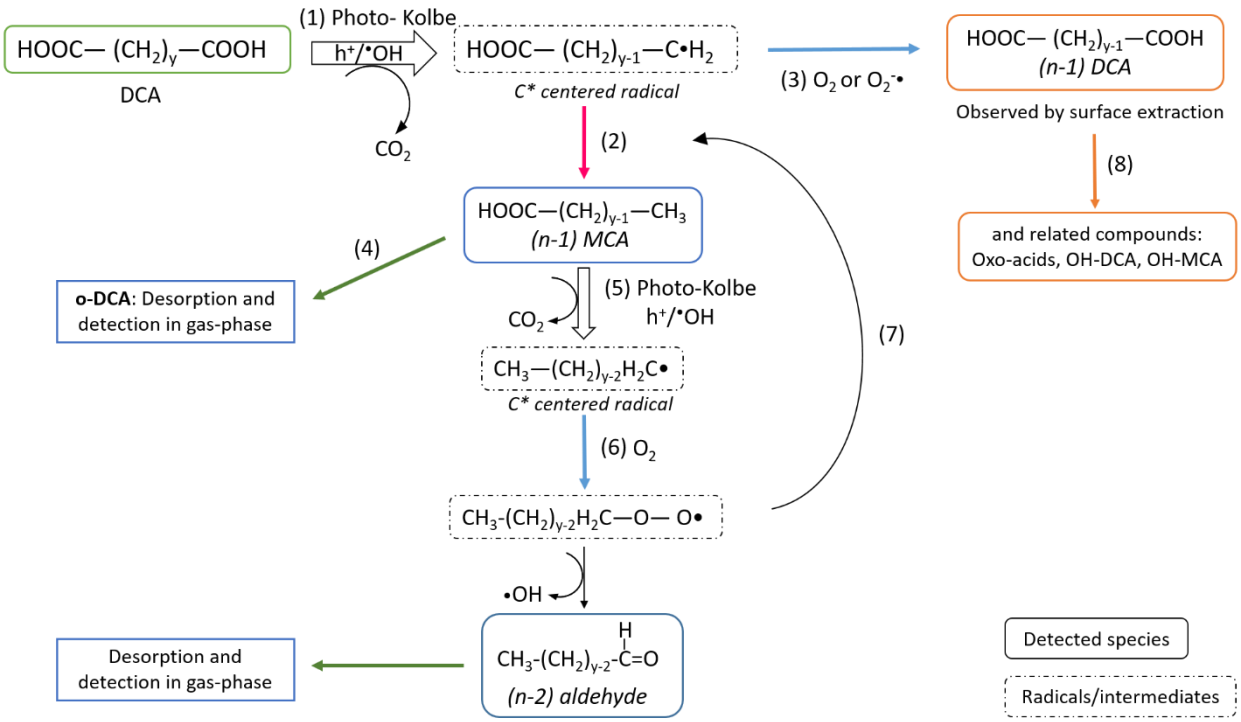

Figure 8: Proposed mechanism for dicarboxylic acids photooxidation on ATD surface under UV-A radiation. Species in solid rectangles were observed by our analytical techniques.

The photooxidation of dicarboxylic acids is suggested to start with the photo-Kolbe reaction (step 1) forming a C-centered alkyl radical and CO_2, with decarboxylation being the first and limiting step. The difference in the adsorption mode is suggested to explain the alternation in the reactivity of DCAs; the monodentate geometry of odd-carbon DCAs makes one carboxylic group weakly bounded and more susceptible to the attack of oxidizing agents such as h_{vb}^+ and radicals (Sun et al., 2014). The bidentate bridging mode, on the other hand, should disfavor the cleavage of the α-carbon bound resulting in less reactivity for even-carbon diacids.

After decarboxylation, the alkyl radical can react either by abstracting an H atom from another organic molecule or surface species, or with O_2. The step 2 (H-abstraction by the alkyl radical) will lead to the $C_{(n-1)}$ MCA observed mostly for the odd-DCA, and the reaction with oxygen (step 3) gives the $C_{(n-1)}$ DCA (Dolamic and Bürgi, 2007). The adsorption/desorption equilibrium determines the partition of the product in the gas/surface phases. For odd-DCA, the decarboxylation is faster than for even-DCA, and the $C_{(n-1)}$ MCA is abundant enough to be released and detected in the gas-phase (step 4). For the even-DCA, the $C_{(n-1)}$ MCA is scarce, and once it is formed, it proceeds to next oxidation steps.

The monocarboxylic acid, in turn, continues the oxidation process, undergoing decarboxylation and, once again, forming alkyl radicals (step 5) which can react with O_2 resulting in peroxyl radicals (step 6) that will lead to carbonylated compounds. The arrow in step 7 represents this pathway can occur successively with each of the intermediates leading to the formation of (n-1) products at each stage. The higher volatility of aldehydes and

formic acid favor their desorption from the surface and explains why they are overwhelmingly detected in the gas-phase.

For a didactic question, the mechanism was depicted in Figure 8 by separating two reactional pathways, one that leads to the gas-phase products (blue rectangles) and the other that results in surface-sorbed compounds (orange rectangles). However, the $C_{(n-1)}$ DCAs observed on the dust surface are also liable to undergo the same kind of reactions as the starting DCA contributing to the products detected on the gas-phase. Moreover, similar to the reaction shown in step 6, after the first decarboxylation, and reaction with O_2 (step 3), the alkyl peroxy radicals (R-O-O•) can lead to oxo acids (step 8), as R, in this case, still has another carboxylic group, as shown as follows on Reactions R1– R4).

$$R\bullet + O_2 \rightarrow R\text{-}O\text{-}O\bullet \quad \text{R1}$$

$$R\text{-}O\text{-}O\bullet + RH \rightarrow ROOH + R\bullet \quad \text{R2}$$

$$ROOH \rightarrow R\text{-}O\bullet + \bullet OH \quad \text{R3}$$

$$R\text{-}O\bullet + O_2 \rightarrow RCHO + HO_2\bullet \quad \text{R4}$$

If R• is formed from the DCA, RCHO is an oxo-acid: HOOC-CH_2(n)-CHO

If R• is formed from the MCA, RCHO is an aldehyde.

The diversity concerning dust particles components behavior punctuates the complexity of the process and emphasizes the importance of the investigation of natural and complex samples where synergy effects among constituent materials can modify the expected results for single components systems. Styler and Donaldson discussed in their study of oxalic acid decomposition on different mineral proxies (Styler and Donaldson, 2012), that the heterogeneous reactivity of realistic dust has contributions of both iron and titanium oxides photochemistry. According to their observations, the reactivity of each semiconductor can be influenced by environmental conditions, for instance, the presence of O_2 decreased the importance of iron-mediated process whereas it enhanced the reactivity for pure TiO_2.

The same comment holds when we compare our results with the studies by Sun et al. (2014), and by Dolamic and Burgui, (2007) who have investigated the photocatalytic degradation of dicarboxylic acids aqueous solutions on TiO_2. Although these studies bring similar and useful mechanistic insights, regarding the products, both reported only acids (mono and dicarboxylic); whereas, in this study, we observed a greater variety of products, notably carbonyl compounds (aldehydes / ketones) in the gas-phase and oxygenated and hydroxylated substituted products in the particulate phase.

From the atmospheric point of view, the emission of carbonyl compounds is relevant since they are photoactive and contribute to the formation of radicals that will participate in the bulk gas-phase chemistry (Mellouki et al., 2015). For instance, carbonyls are fundamental in the formation of HO_x species; additionally, reactions of

carbonyls with Br and Cl are also major sources of HBr and HCl in the upper troposphere and lower stratosphere (Lary and Shallcross, 2000).

3.6 Conclusions and Atmospheric Implications

In this study, we have shown that photo-induced reactions can take place on realistic dust surfaces coated with organic compounds. Our results show that when starting with a single dicarboxylic acid, the particles catalyzed chemical reactions producing a complex mixture of organic compounds upon irradiation. We have characterized the products of this photooxidation process presenting both the volatile compounds that are emitted in the gas-phase and the low volatility ones which stay adsorbed on dust. Moreover, it was proposed a mechanism that agrees and summarizes experimental observations. Surprisingly, the reactivity of the dicarboxylic acids presented an alternation concerning the number of carbons of the chain, and the odd-DCAs exhibited greater reactivity than the even ones. Although unexpected, the alternation of properties (physical and also chemical) has already been observed regarding to DCAs.

About the products detected adsorbed on the solid phase, it is emphasized the presence of highly oxygenated and substituted products that is especially important because of their higher polarity and affinity with water. Keskinen et al. (2014) measured the hygroscopicity of ATD seed particles exposed to SOA from the ozonolysis of α-pinene and found an increase by a factor of four for 100-150 nm particles (Keskinen et al., 2014). Their results highlight the effect of organic matter heterogeneous coating on solid particles hygroscopic properties and cloud droplet activation. Sullivan and Pradher, by contrast, commented that the association of DCA acids with mineral dust or sea salt could form insoluble complexes possibly diminishing cloud activation properties of those particles (Sullivan and Prather, 2007).

In addition, studies of ice nucleation (IN) have shown that particle coatings decreased IN ability compared to pure ATD (Niedermeier et al., 2010). Möhler and coworkers (Möhler et al., 2008) have investigated the ice nucleation efficiency of ATD particles coated by condensation of semi-volatile products from the reaction of α-pinene with ozone and found out that these SOA compounds lowered or even suppressed, in certain conditions, the heterogeneous ice nucleation potential of dust. The influence of organic matter oxidation state on CCN and IN activity is not yet a consensus in the scientific community, and more mechanistic understanding is needed. However, it is broadly recognized that organic compounds coating insoluble dust cores affect their CCN and IN potential.

Water is known to play an important role in photocatalytic reactions efficiently generating OH-radicals and changing selectivity towards total oxidation (Herrmann, 2001) but also competing for reactive sites. We did not investigate the direct influence of water or relative humidity, although in our procedure no effort was made to eliminate all the water used in the coating process; and therefore, water molecules must have remained on the

surface, especially those strongly bonded (by hydrogen bonds). However, a systematic evaluation of the role of relative humidity might be interesting and indeed, recommended for future studies.

Overall, the results obtained herein agree with other studies (Kawamura and Bikkina, 2016), (Helmi Rozaini, 2012), (Kawamura and Sakaguchi, 1999) suggesting that longer chain DCA are precursors of shorter diacids. We could wonder that heterogeneous photochemical processing might be an important pathway for small DCA formation.

In conclusion, this study revealed the role of irradiation in the aging of organic coated mineral surfaces. The chemical and physical properties of mineral aerosols can be substantially influenced by the photochemical production of small diacids and the evolution of their intermediates. Furthermore, the dust potential to induce reactions that lead to the oxidation of organic acids and the release of oxygenated volatile organic compounds to the gas-phase could alter atmospheric composition in the surroundings of a dust plume.

Acknowledgments

The authors gratefully acknowledge the Brazilian National Council for Scientific and Technological Development−CNPq, Brazil for the financial support (Ph.D. fellowship of M. P.), the Marie Curie International Research Staff Exchange project MARSU (Grant 690958), and the Region Auvergne Rhone Alpes.

Supplement related to this article is available.

Competing interests. The authors declare that they have no conflict of interest

References

Bilde, M., Barsanti, K., Booth, M., Cappa, C.D., Donahue, N.M., Emanuelsson, E.U., McFiggans, G., Krieger, U.K., Marcolli, C., Topping, D., Ziemann, P., Barley, M., Clegg, S., Dennis-Smither, B., Hallquist, M., Hallquist, Å.M., Khlystov, A., Kulmala, M., Mogensen, D., Percival, C.J., Pope, F., Reid, J.P., Ribeiro da Silva, M.A. V., Rosenoern, T., Salo, K., Soonsin, V.P., Yli-Juuti, T., Prisle, N.L., Pagels, J., Rarey, J., Zardini, A.A., Riipinen, I., 2015. Saturation Vapor Pressures and Transition Enthalpies of Low-Volatility Organic Molecules of Atmospheric Relevance: From Dicarboxylic Acids to Complex Mixtures. Chem. Rev. 115, 4115–4156. https://doi.org/10.1021/cr5005502

Brüggemann, M., Hayeck, N., Bonnineau, C., Pesce, S., Alpert, P.A., Perrier, S., Zuth, C., Hoffmann, T., Chen, J., George, C., 2017. Interfacial photochemistry of biogenic surfactants: a major source of abiotic volatile organic compounds. Faraday Discuss. 200, 59–74. https://doi.org/10.1039/C7FD00022G

Carlos-Cuellar, S., Li, P., Christensen, A.P., Krueger, B.J., Burrichter, C., Grassian, V.H., 2003. Heterogeneous Uptake Kinetics of Volatile Organic Compounds on Oxide Surfaces Using a Knudsen Cell Reactor: Adsorption of Acetic Acid, Formaldehyde, and Methanol on α-Fe 2 O 3 , α-Al 2 O 3 , and SiO 2. J. Phys. Chem. A 107, 4250–4261. https://doi.org/10.1021/jp0267609

Charbouillot, T., Gorini, S., Voyard, G., Parazols, M., Brigante, M., Deguillaume, L., Delort, A.M., Mailhot, G., 2012. Mechanism of carboxylic acid photooxidation in atmospheric aqueous phase: Formation, fate and reactivity. Atmos. Environ. https://doi.org/10.1016/j.atmosenv.2012.03.079

Chebbi, A., Carlier, P., 1996. Carboxylic acids in the troposphere, occurrence, sources, and sinks: A review. Atmos. Environ. 30, 4233–4249. https://doi.org/10.1016/1352-2310(96)00102-1

Chen, H., Nanayakkara, C.E., Grassian, V.H., 2012. Titanium dioxide photocatalysis in atmospheric chemistry. Chem. Rev. 112, 5919–5948. https://doi.org/10.1021/cr3002092

de Gouw, J., Warneke, C., 2007. Measurements of volatile organic compounds in the earth's atmosphere using proton-transfer-reaction mass spectrometry. Mass Spectrom. Rev. 26, 223–257. https://doi.org/10.1002/mas.20119

Dolamic, I., Bürgi, T., 2007. Photocatalysis of dicarboxylic acids over TiO2: An in situ ATR-IR study. J. Catal. 248, 268–276. https://doi.org/10.1016/j.jcat.2007.03.020

Dolamic, I., Bürgi, T., 2006. Photoassisted Decomposition of Malonic Acid on TiO 2 Studied by in Situ Attenuated Total Reflection Infrared Spectroscopy. J. Phys. Chem. B 110, 14898–14904. https://doi.org/10.1021/jp0616967

Fairhurst, M.C., Ezell, M.J., Kidd, C., Lakey, P.S.J., Shiraiwa, M., Finlayson-Pitts, B.J., 2017. Kinetics, mechanisms and ionic liquids in the uptake of n-butylamine onto low molecular weight dicarboxylic acids. Phys. Chem. Chem. Phys. 19, 4827–4839. https://doi.org/10.1039/C6CP08663B

Falkovich, A.H., Schkolnik, G., Ganor, E., Rudich, Y., 2004. Adsorption of organic compounds pertinent to urban environments onto mineral dust particles. J. Geophys. Res. 109, D02208. https://doi.org/10.1029/2003JD003919

Formenti, P., Schütz, L., Balkanski, Y., Desboeufs, K., Ebert, M., Kandler, K., Petzold, A., Scheuvens, D., Weinbruch, S., Zhang, D., 2011. Recent progress in understanding physical and chemical properties of African and Asian mineral dust. Atmos. Chem. Phys. 11, 8231–8256. https://doi.org/10.5194/acp-11-8231-2011

George, C., Ammann, M., D'Anna, B., Donaldson, D.J., Nizkorodov, S. a., 2015. Heterogeneous Photochemistry in the Atmosphere. Chem. Rev. 115, 4218–4258. https://doi.org/10.1021/cr500648z

Hartungen, E. Von, Wisthaler, A., Mikoviny, T., Jaksch, D., Boscaini, E., Dunphy, P.J., Märk, T.D., 2004. Proton-transfer-reaction mass spectrometry (PTR-MS) of carboxylic acids: Determination of Henry's law constants and axillary odour investigations. Int. J. Mass Spectrom. 239, 243–248. https://doi.org/10.1016/j.ijms.2004.09.009

Helmi Rozaini, M.Z., 2012. The Chemistry of Dicarboxylic Acids in the Atmospheric Aerosols, in: Atmospheric Aerosols - Regional Characteristics - Chemistry and Physics. InTech. https://doi.org/10.5772/50127

Herrmann, J.-M., 2010. Fundamentals and misconceptions in photocatalysis. J. Photochem. Photobiol. A Chem. 216, 85–93. https://doi.org/10.1016/j.jphotochem.2010.05.015

Herrmann, J.-M., 2001. Active Agents in Heterogeneous Photocatalysis: Atomic Oxygen Species vs. OH. Radicals: Related Quantum Yields. Helv. Chim. Acta 84, 2731. https://doi.org/10.1002/1522-2675(20010919)84:9<2731::AID-HLCA2731>3.0.CO;2-L

Jammoul, A., Gligorovski, S., George, C., D'Anna, B., 2008. Photosensitized heterogeneous chemistry of ozone on organic films. J. Phys. Chem. A 112, 1268–1276. https://doi.org/10.1021/jp074348t

Kawamura, K., Bikkina, S., 2016. A review of dicarboxylic acids and related compounds in atmospheric aerosols: Molecular distributions, sources and transformation. Atmos. Res. https://doi.org/10.1016/j.atmosres.2015.11.018

Kawamura, K., Ikushima, K., 1993. Seasonal Changes in the Distribution of Dicarboxylic Acids in the Urban Atmosphere. Environ. Sci. Technol. 27, 2227–2235. https://doi.org/10.1021/es00047a033

Kawamura, K., Kasukabe, H., Barrie, L.A., 1996. Source and reaction pathways of dicarboxylic acids, ketoacids and dicarbonyls in arctic aerosols: One year of observations. Atmos. Environ. 30, 1709–1722. https://doi.org/10.1016/1352-2310(95)00395-9

Kawamura, K., Sakaguchi, F., 1999. Molecular distributions of water soluble dicarboxylic acids in marine aerosols over the Pacific Ocean including tropics. J. Geophys. Res. Atmos. 104, 3501–3509. https://doi.org/10.1029/1998JD100041

Kawamura, K., Yasui, O., 2005. Diurnal changes in the distribution of dicarboxylic acids, ketocarboxylic acids and dicarbonyls in the urban Tokyo atmosphere. Atmos. Environ. 39, 1945–1960. https://doi.org/10.1016/j.atmosenv.2004.12.014

Keskinen, H., Kortelainen, A.M., Jaatinen, A., Yli-Pirilä, P., Joutsensaari, J., Romakkaniemi, S., Hao, L.Q., Miettinen, P., Virtanen, A., Worsnop, D.R., Laaksonen, A., Smith, J.N., Torvela, T., Laaksonen, A., Worsnop, D.R., Smith, J.N., Romakkaniemi, S., 2014. Increased hygroscopicity of Arizona Test Dust seeds by secondary organic aerosol coating from α-pinene ozonolysis. Boreal Environ. Res. 19 (suppl., 182–190.

Lary, D.J., Shallcross, D.E., 2000. Central role of carbonyl compounds in atmospheric chemistry. J. Geophys. Res. Atmos. 105, 19771–19778. https://doi.org/10.1029/1999JD901184

Li, P., Perreau, K.A., Covington, E., Song, C.H., Carmichael, G.R., Grassian, V.H., 2001. Heterogeneous reactions of volatile organic compounds on oxide particles of the most abundant crustal elements: Surface reactions of acetaldehyde, acetone, and propionaldehyde on SiO2, Al2O3, Fe2O3, TiO2 , and CaO. J. Geophys. Res. Atmos. 106, 5517–5529. https://doi.org/10.1029/2000JD900573

Mellouki, A., Wallington, T.J., Chen, J., 2015. Atmospheric Chemistry of Oxygenated Volatile Organic Compounds: Impacts on Air Quality and Climate. Chem. Rev. 115, 3984–4014. https://doi.org/10.1021/cr500549n

Möhler, O., Benz, S., Saathoff, H., Schnaiter, M., Wagner, R., Schneider, J., Walter, S., Ebert, V., Wagner, S., 2008. The effect of organic coating on the heterogeneous ice nucleation efficiency of mineral dust aerosols. Environ. Res. Lett. 3, 025007. https://doi.org/10.1088/1748-9326/3/2/025007

Ndour, M., Conchon, P., D'Anna, B., Ka, O., George, C., 2009. Photochemistry of mineral dust surface as a potential atmospheric renoxification process. Geophys. Res. Lett. 36, L05816. https://doi.org/10.1029/2008GL036662

Niedermeier, D., Hartmann, S., Shaw, R.A., Covert, D., Mentel, T.F., Schneider, J., Poulain, L., Reitz, P., Spindler, C., Clauss, T., Kiselev, A., Hallbauer, E., Wex, H., Mildenberger, K., Stratmann, F., 2010. Heterogeneous freezing of droplets with immersed mineral dust particles – measurements and parameterization. Atmos. Chem. Phys. 10, 3601–3614. https://doi.org/10.5194/acp-10-3601-2010

Ohtani, B., 2010. Photocatalysis A to Z—What we know and what we do not know in a scientific sense. J. Photochem. Photobiol. C Photochem. Rev. 11, 157–178. https://doi.org/10.1016/j.jphotochemrev.2011.02.001

Pan, X., Uno, I., Wang, Zhe, Nishizawa, T., Sugimoto, N., Yamamoto, S., Kobayashi, H., Sun, Y., Fu, P., Tang, X., Wang, Zifa, 2017. Real-time observational evidence of changing Asian dust morphology with the mixing of heavy anthropogenic pollution. Sci. Rep. 7, 335. https://doi.org/10.1038/s41598-017-00444-w

Pavuluri, C.M., Kawamura, K., Mihalopoulos, N., Swaminathan, T., 2015. Laboratory photochemical processing of aqueous aerosols: formation and degradation of dicarboxylic acids, oxocarboxylic acids and α-dicarbonyls. Atmos. Chem. Phys. 15, 7999–8012. https://doi.org/10.5194/acp-15-7999-2015

Ponczek, M., George, C., 2018. Kinetics and Product Formation during the Photooxidation of Butanol on Atmospheric Mineral Dust. Environ. Sci. Technol. 52, 5191–5198. https://doi.org/10.1021/acs.est.7b06306

Romanias, M.N., Zeineddine, M.N., Gaudion, V., Lun, X., Thevenet, F., Riffault, V., 2016. Heterogeneous Interaction of Isopropanol with Natural Gobi Dust. Environ. Sci. Technol. 50, 11714–11722. https://doi.org/10.1021/acs.est.6b03708

Russell, L.M., Maria, S.F., Myneni, S.C.B., 2002. Mapping organic coatings on atmospheric particles. Geophys. Res. Lett. 29, 26-1-26–4. https://doi.org/10.1029/2002GL014874

Styler, S.A., Donaldson, D.J., 2012. Heterogeneous Photochemistry of Oxalic Acid on Mauritanian Sand and Icelandic Volcanic Ash. Environ. Sci. Technol. 46, 8756–8763. https://doi.org/10.1021/es300953t

Styler, S.A., Donaldson, D.J., 2011. Photooxidation of atmospheric alcohols on laboratory proxies for mineral dust. Environ. Sci. Technol. 45, 10004–12. https://doi.org/10.1021/es202263q

Styler, S.A., Myers, A.L., Donaldson, D.J., 2013. Heterogeneous Photooxidation of Fluorotelomer Alcohols: A New Source of Aerosol-Phase Perfluorinated Carboxylic Acids. Environ. Sci. Technol. 47, 6358–6367. https://doi.org/10.1021/es4011509

Sullivan, R.C., Guazzotti, S.A., Sodeman, D.A., Prather, K.A., 2007. Direct observations of the atmospheric processing of Asian mineral dust. Atmos. Chem. Phys. 7, 1213–1236. https://doi.org/10.5194/acp-7-1213-2007

Sullivan, R.C., Prather, K.A., 2007. Investigations of the Diurnal Cycle and Mixing State of Oxalic Acid in Individual Particles in Asian Aerosol Outflow. Environ. Sci. Technol. 41, 8062–8069. https://doi.org/10.1021/es071134g

Sun, Y., Chang, W., Ji, H., Chen, C., Ma, W., Zhao, J., 2014. An Unexpected Fluctuating Reactivity for Odd and Even Carbon Numbers in the TiO 2 -Based Photocatalytic Decarboxylation of C2-C6 Dicarboxylic Acids. Chem. - A Eur. J. 20, 1861–1870. https://doi.org/10.1002/chem.201303236

Tang, M., Cziczo, D.J., Grassian, V.H., 2016. Interactions of Water with Mineral Dust Aerosol: Water Adsorption, Hygroscopicity, Cloud Condensation, and Ice Nucleation. Chem. Rev. 116, 4205–4259. https://doi.org/10.1021/acs.chemrev.5b00529

Thalladi, V.R., Nüsse, M., Boese, R., 2000. The Melting Point Alternation in α , ω -Alkanedicarboxylic Acids †. J. Am. Chem. Soc. 122, 9227–9236. https://doi.org/10.1021/ja0011459

Usher, C.R., Michel, A.E., Grassian, V.H., 2003. Reactions on Mineral Dust. Chem. Rev. 103, 4883–4939. https://doi.org/10.1021/cr020657y

Wang, X.K., Rossignol, S., Ma, Y., Yao, L., Wang, M.Y., Chen, J.M., George, C., Wang, L., 2016. Molecular characterization of atmospheric particulate organosulfates in three megacities at the middle and lower reaches of the Yangtze River. Atmos. Chem. Phys. 16, 2285–2298. https://doi.org/10.5194/acp-16-2285-2016

Yang, L., Ray, M.B., Yu, L.E., 2008. Photooxidation of dicarboxylic acids—Part II: Kinetics, intermediates and field observations. Atmos. Environ. 42, 868–880. https://doi.org/10.1016/j.atmosenv.2007.10.030

Yuan, B., Koss, A.R., Warneke, C., Coggon, M., Sekimoto, K., De Gouw, J.A., 2017. Proton-Transfer-Reaction Mass Spectrometry: Applications in Atmospheric Sciences. Chem. Rev. 117, 13187–13229. https://doi.org/10.1021/acs.chemrev.7b00325

Zhang, H., Xie, C., Liu, Z., Gong, J., Bao, Y., Zhang, M., Hao, H., Hou, B., Yin, Q., 2013. Identification and Molecular Understanding of

the Odd–Even Effect of Dicarboxylic Acids Aqueous Solubility. Ind. Eng. Chem. Res. 52, 18458–18465. https://doi.org/10.1021/ie4030837

Zhang, H., Yin, Q., Liu, Z., Gong, J., Bao, Y., Zhang, M., Hao, H., Hou, B., Xie, C., 2014. An odd–even effect on solubility of dicarboxylic acids in organic solvents. J. Chem. Thermodyn. 77, 91–97. https://doi.org/10.1016/j.jct.2014.05.009

Zhao, Y., Fairhurst, M.C., Wingen, L.M., Perraud, V., Ezell, M.J., Finlayson-Pitts, B.J., 2017. New insights into atmospherically relevant reaction systems using direct analysis in real-time mass spectrometry (DART-MS). Atmos. Meas. Tech. 10, 1373–1386. https://doi.org/10.5194/amt-10-1373-2017